Asymmetric Splitting of an Antiferromagnetic Resonance via Quartic Exchange Interactions in Multiferroic Hexagonal $HoMnO_3$

N. J. Laurita,[1] Yi Luo,[1] Rongwei Hu,[2] Meixia Wu,[2] S. W. Cheong,[2] O. Tchernyshyov,[1] and N. P. Armitage[1]
[1]*The Institute for Quantum Matter, Department of Physics and Astronomy, The Johns Hopkins University, Baltimore, Maryland 21218, USA*
[2]*Rutgers Center For Emergent Materials, Department of Physics and Astronomy, Rutgers University, Piscataway, New Jersey 08854, USA*

(Received 26 May 2017; revised manuscript received 10 October 2017; published 1 December 2017)

The symmetric splitting of two spin-wave branches in an antiferromagnetic resonance (AFR) experiment has been an essential measurement of antiferromagnets for over half a century. In this work, circularly polarized time-domain THz spectroscopy experiments performed on the low symmetry multiferroic hexagonal $HoMnO_3$ reveal an AFR of the Mn sublattice to split asymmetrically in an applied magnetic field, with an ≈50% difference in g factors between the high and low energy branches of this excitation. The temperature dependence of the g factors, including a drastic renormalization at the Ho spin ordering temperature, reveals this asymmetry to unambiguously stem from Ho-Mn interactions. Theoretical calculations demonstrate that the AFR asymmetry is not explained by conventional Ho-Mn exchange mechanisms alone and is only reproduced if quartic spin interactions are also included in the spin Hamiltonian. Our results provide a paradigm for the optical study of such novel interactions in hexagonal manganites and low symmetry antiferromagnets in general.

DOI: 10.1103/PhysRevLett.119.227601

Antiferromagnetic resonance (AFR) has been, perhaps, the most essential property of antiferromagnets since the earliest description by Kittel over half a century ago [1]. In an AFR experiment, two spin-wave branches, each active to a different helicity of circularly polarized light, symmetrically split in an applied magnetic field. However, changes to this phenomena may occur in low symmetry environments, as interactions between localized spins in magnetic insulators are heavily influenced by the symmetry of the crystal structure in which they are embedded. The hexagonal rare-earth manganites (h-$RMnO_3$) are prime examples of materials whose low symmetry results in remarkable physical behavior [2], including multiferroism and exceptionally strong magnetoelectric coupling [3]. Magnetism in these systems consists of both rare-earth and manganese magnetic moments, which lie in orthogonal directions due to crystalline anisotropy [4]. Interactions between these moments has been a topic of intense investigation [4–8] as such couplings are thought to drive magnetic transitions [9] and mediate magnetoelectric phenomena [10,11]. However, the exchange mechanism between R-Mn spins has remained elusive, as their orthogonality suggests a less conventional interaction than the Heisenberg exchange in the equilibrium spin configuration.

Of these materials, hexagonal $HoMnO_3$ (HMO) possesses the largest effective rare-earth magnetic moment and is, thus, ideal for studying magnetic exchange in these systems [3,12–15]. The hexagonal crystal structure of HMO (Fig. 1) consists of alternating layers of corner sharing MnO_5 bipyramids and Ho ions which are stacked along the c axis [16]. At the ferroelectric transition, $T_c = 875$ K, the MnO_5 bipyramids buckle [17–19] reducing the symmetry to the noncentrosymmetric polar space group $P6_3cm$ with Ho ions occupying two symmetry distinct positions of the crystal lattice. The $S_{Mn} = 2$ spins form a two-dimensional frustrated triangular lattice which orders at $T_N \approx 75$ K in a 120° structure with symmetry $P6'_3c'm$ [20–25]. Two additional zero field Mn sublattice transitions occur at $T_{SR} \approx 40$ K ($P6'_3cm'$) and at $T_{Ho} \approx 5$ K ($P6_3cm$), in which the Mn spins rotate by 90° within the

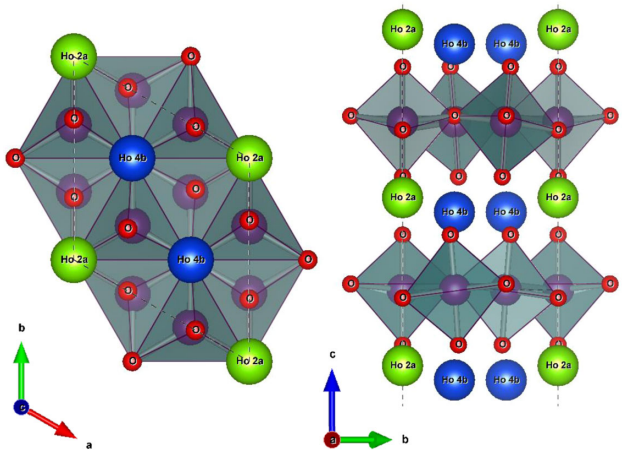

FIG. 1. Crystal structure of HMO in the ferroelectric phase ($T < T_c = 875$ K) with views along the (left) c axis and (right) a axis, respectively. In this phase, the Ho^{+3} ions (green and blue spheres) lie in symmetrically distinct positions of the lattice resulting in a finite ferroelectric moment along the c axis.

basal plane. The ordering of the Ho sublattices is less understood [4,20–27]; however, it is expected that the $S_{\mathrm{Ho}} = 2$ spins order antiferromagnetically along the c axis due to uniaxial anisotropy [4], with experimental evidence suggesting that magnetization of at least one of the Ho sublattices onsets near T_{SR} [4,27] and some form of long range order existing below T_{Ho}.

Interactions between R and Mn moments in hexagonal manganites can be probed by examining the spin excitations of the Mn sublattice, whose minimal spin Hamiltonian is given by

$$H = J\sum_{\langle ij\rangle}\mathbf{S}_i\cdot\mathbf{S}_j + \Delta\sum_i (S_i^z)^2 - g\mu_B\mathbf{B}\cdot\sum_i \mathbf{S}_i, \quad (1)$$

where J is the Heisenberg exchange, Δ is the planar anisotropy, $\mathbf{B}\|c$ is the applied magnetic field, $g = 2$ is the Mn g factor, and the sum is over neighboring pairs [23,28]. The ground state of the Mn sublattice is a 120° ordered AF. In the $\vec{k}\to 0$ limit (applicable to our optical measurements) the low energy spectrum consists of a Goldstone mode and a gapped AFR [28]. In the weak field limit, valid for fields $H < S_{\mathrm{Mn}}J \approx 40$ T in HMO, the energies of the AFR are given by

$$\hbar\omega_{\pm}(B) = \hbar\omega(0) \pm g_{\mathrm{eff}}\mu_B B, \qquad \hbar\omega(0) = 3S\sqrt{J\Delta}, \quad (2)$$

revealing two modes which split symmetrically in field with $g_{\mathrm{eff}} = g/(2 + 4\Delta/9J)$ [29] [see Eqs. (8–12) of Sec. III in the Supplemental Material (SM) for derivation [30]]. Note that even for small anisotropy, g_{eff} is approximately half the bare ionic value. This is a particular feature of the 120° ordered AF which arises due to the low symmetry of the ordered state resulting in a not well defined z angular momentum quantum number. With exchange and anisotropy found to be $J = 2.44$ meV and $\Delta = 0.38$ meV, respectively, in HMO [23], one expects $g_{\mathrm{eff}} = 0.97$ from Eq. (2). However, in actuality much larger g factors are observed at low temperatures in hexagonal manganites [7,29]. This has been explained by introducing an additional Heisenberg exchange interaction which ferromagnetically couples R spins to the finite S_z of the Mn AFR modes into Eq. (1) [7]. However, such a coupling is expected to vanish in the ground state due to the orthogonality of spins, leaving the dominant equilibrium R-Mn spin interaction unresolved.

In this Letter, we present a systematic study of the low energy optical response of HMO via high resolution time-domain terahertz spectroscopy (TDTS). We demonstrate that the Mn AFR possesses distinct selection rules to circularly polarized light, which allows our experiments to resolve the field dependent splitting of the AFR in weak magnetic fields with high precision. The AFR is found to unexpectedly split asymmetrically in magnetic fields. Careful study of the temperature dependence of this asymmetry unambiguously demonstrates the effect to stem from R-Mn interactions. Theoretical investigation concludes that the asymmetry is not explained by conventional R-Mn exchange mechanisms alone and is only reproduced if novel quartic spin interactions are also included in the spin Hamiltonian. The potential for such interactions in other hexagonal manganites is discussed.

Single crystals of HMO were grown via the optical floating zone method. Two samples with the orientations $[-1, 1, 0]$ ($d = 670$ μm) and $[0,0,1]$ ($d = 590$ μm) normal to the sample surface were measured in this study. TDTS transmission experiments were performed using a home-built spectrometer [31] in magnetic fields up to $6T$ in Faraday geometry ($\vec{k}_{\mathrm{THz}}\|\vec{\mathrm{H}}_{\mathrm{dc}}$). Via a coupling of the THz fields to both electric and magnetic dipole transitions of the sample, TDTS accesses the sample's electromagnetic response with exceptional resolution from 0.2–2 THz.

Figure 2 displays image plots of the imaginary, or dissipative, part of the complex index of refraction, $\tilde{n} = n + ik$, of HMO for the orientations (a) $\vec{\mathrm{h}}_{\mathrm{ac}}\|c$ and (b) $\vec{\mathrm{h}}_{\mathrm{ac}}\perp c$, respectively, (full data set in Sec. IV of the SM [30]). One can show that the axial symmetry of the lattice constrains the zero field linear response such that only these two orientations give unique responses [32]. The spectra are in excellent agreement with previous studies [7,33]. Many of the features seen in Fig. 2 can be attributed to crystal field transitions of the Ho^{+3} ($^5I_8$) ions, which have been previously discussed in the context of a number of compounds [34–40]. Several of the more prominent crystal field levels are labeled in Fig. 2 and discussed in detail in

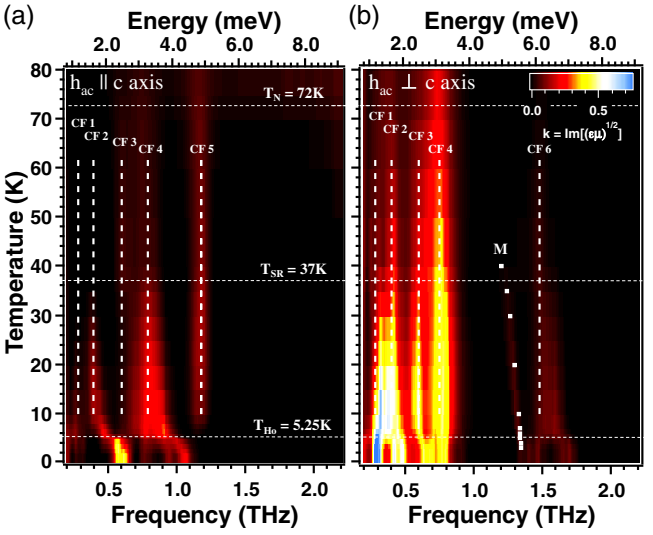

FIG. 2. Image plots of the imaginary part of the index of refraction as a function of temperature and frequency for the orientations (a) $\vec{\mathrm{h}}_{\mathrm{ac}}\|c$ and (b) $\vec{\mathrm{h}}_{\mathrm{ac}}\perp c$, respectively. Horizontal dashed lines denote the three zero field transition temperatures while vertical dashed lines label the more prominent Ho crystal field (CF) excitations identified at temperatures $T \geq T_{\mathrm{Ho}}$. The excitation labeled M is the AFR of the Mn sublattice whose resonant frequency is marked by white squares.

Sec. IV of the SM (see Table I) [30]. Abrupt changes in the spectra, including a previously undiscovered dramatic renormalization of the crystal field excitation energies at ≈5 K, identify the three zero field magnetic transitions at $T_N = 72$ K, $T_{SR} = 37$ K, and $T_{Ho} = 5.25$ K. Here, we focus on the AFR of the Mn sublattice which is labeled "M" in Fig. 2. In order to extract the dynamical properties of this mode, the spectra were fit with a Drude-Lorentz oscillator on a linear background to account for neighboring crystal field levels. White squares in Fig. 2 mark the extracted resonant frequencies of the Mn AFR.

Measurements were then performed as a function of the magnetic field to investigate the field dependent splitting of the AFR. The hexagonal symmetry of HMO along with the $\mathcal{T}$ symmetry breaking under the applied field constrains the linear response transmission matrix [32,41] such that it must be fully antisymmetric in the linear basis

$$\tilde{T}_{\text{linear}} = \begin{bmatrix} \tilde{T}_{xx} & \tilde{T}_{xy} \\ -\tilde{T}_{xy} & \tilde{T}_{xx} \end{bmatrix}. \quad (3)$$

Such a fully antisymmetric transmission matrix can be diagonalized by a circular basis transformation as

$$\tilde{T}_{\text{circular}} = \begin{bmatrix} \tilde{T}_{xx} + i \cdot \tilde{T}_{xy} & 0 \\ 0 & \tilde{T}_{xx} - i \cdot \tilde{T}_{xy} \end{bmatrix} = \begin{bmatrix} \tilde{T}_r & 0 \\ 0 & \tilde{T}_l \end{bmatrix}, \quad (4)$$

where $\tilde{T}_l$ and $\tilde{T}_r$ refer to the transmission of left-hand and right-hand circularly polarized light, the eigenpolarizations, respectively. The above analysis suggests that experiments performed in Faraday geometry are best understood in the circular basis (see Sec. I of the SM for further details [30]). TDTS measurements performed here utilized a rotating polarizer technique, which allows for measurement of the sample's response to two polarization directions simultaneously and, thus, conversion to the circular basis [42].

Figures 3(a) and 3(b) display image plots of the dissipative part of the index of refraction as a function of the magnetic field at 20 K for right-hand and left-hand circular polarizations, respectively. The excitation at ≈1.3 THz which linearly varies with the magnetic field is the AFR of the Mn sublattice. One can immediately see that the two branches of the AFR possess distinct selection rules to right-hand and left-hand circular polarizations. Such a partitioning of the AFR allows unique access to the splitting of this mode in weak magnetic fields, within the low field "intermediate" phase of HMO, where the two branches would, otherwise, be highly overlapping in the linear basis. In a similar manner as the zero field data, these spectra were fit to extract the magnetic field dependent dynamical properties of the AFR. White triangles in Fig. 3 mark the resonant frequency of the AFR at fields in which it is well defined.

The g factors of the AFR can be found by fitting the extracted resonant frequencies as a function of the magnetic field. To reiterate, the expectation from Eq. (2) is a symmetric splitting of the two branches with g factors $\approx \pm 1$. Figure 4(a) displays linear fits of the AFR resonant frequencies in weak magnetic fields, within the low field phase of HMO. One can see that g factors are not only large but also unexpectedly asymmetric, with the low energy branch possessing a g factor that is ≈50% greater than that of the high energy branch. This asymmetry extends to negative fields as well, such that the low energy branch always possesses a larger g factor. A remarkable aspect of the data is the kink in the R and L branches as a function of B near zero field. We believe this nonanalyticity results from the manner in which the ground state is selected with a change in sign of the magnetic field as discussed below. The small difference in g factor for the low energy branches between positive and negative fields likely stems from larger error bars in negative fields due to a weak AFR in this orientation. While enhanced g factors have been interpreted via R-Mn spin interactions [7], asymmetry in the field dependent splitting of the AFR has not been reported previously.

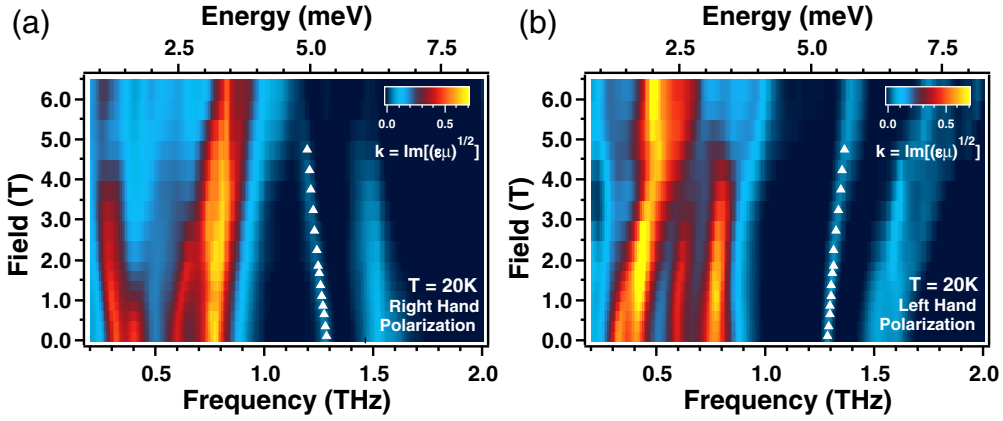

FIG. 3. Field dependence of the imaginary part of the index of refraction of HMO at 20 K for (a) right-hand and (b) left-hand circular polarizations with $H \| c$. The Mn AFR is the linearly varying excitation at ≈1.3 THz, which can be seen to naturally partition into low and high energy branches in the circular basis. White triangles mark the extracted resonant frequencies of the AFR.

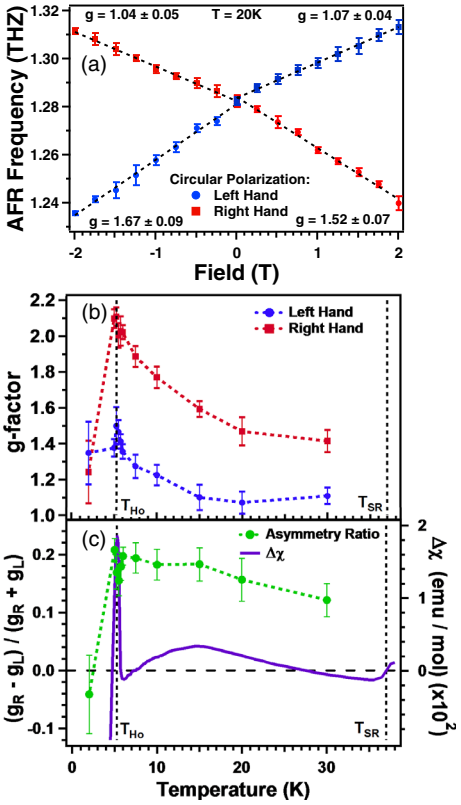

FIG. 4. (a) Resonant frequency of the AFR for both left-hand (blue, circles) and right-hand (red, squares) circular polarizations as a function of the magnetic field at $T = 20$ K. The low energy branch of the AFR possesses a significantly larger g factor than that of the high energy branch, regardless of polarization and field direction. (b) Temperature dependence of the g factors which reveals a significant renormalization at T_{Ho}. (c) Asymmetry ratio of the g factors plotted with $\Delta\chi$, the $H\|c$ magnetic susceptibility after the paramagnetic contribution has been subtracted.

We can ascertain the origin of this asymmetry by examining the temperature dependence of the g factors [Fig. 4(b)]. The g factors increase with decreasing temperature, a trend which is consistent with other hexagonal manganites [29]. However, in HMO we observe a large renormalization of the g factors at T_{Ho}, with increases of $\approx$50% and 35% from 30 K to T_{Ho} in the right-hand and left-hand branches, respectively. This effect can be attributed to a large increase in the effective internal fields near T_{Ho} as the Ho sublattices are more easily magnetized near the transition, consistent with the observed peak in the magnetic susceptibility at T_{Ho} [Fig. 4(c)] [2]. Below the transition, with the Ho sublattices presumably AF ordered, the internal fields are reduced and the g factors return close to their high temperature values (although the error bars at 2 K are large due to overlap with neighboring Ho crystal field levels). Figure 4(c) displays the asymmetry ratio, defined as $(g_R - g_L)/(g_R + g_L)$, along with $\Delta\chi$, the $H\|c$ magnetic susceptibility of HMO after the paramagnetic contribution has been subtracted. We can attribute this susceptibility to stem mainly from Ho magnetism. One can see that the temperature dependence of the asymmetry ratio is in remarkable agreement with the magnetic susceptibility, increasing below T_{SR}, being renormalized at T_{Ho}, and decreasing rapidly at lower temperatures. Such a plot unambiguously demonstrates the g factor asymmetry to be related to Ho-Mn interactions.

To investigate the origin of this asymmetry, we have explored a scenario in which paramagnetic Ho moments generate an effective exchange field on Mn sites. To tilt both AFR branches down, this exchange field $\mathbf{H}_{\mathrm{eff}}$ must be antiparallel to Mn moments, reducing the cost of small deviations from the ordered state. At the same time, it is generated by fluctuating Ho moments whose thermal average $\langle S^z_{\mathrm{Ho}}\rangle = \chi_{\mathrm{Ho}} B$ is proportional to the applied field B and to the Ho magnetic susceptibility χ_{Ho}, which grows as the temperature is lowered toward the Ho ordering at T_{Ho}. In this case, the exchange and anisotropy of Eq. (2) are modified such that they depend linearly on B as

$$J \mapsto J(B) \equiv J + J'B, \qquad \Delta \mapsto \Delta(B) \equiv \Delta + \Delta' B. \tag{5}$$

Then, to the linear order, the energies of the AFR are

$$\hbar\omega_{\pm}(B) = \hbar\omega(0) + \hbar\omega(0)\left(\frac{J'}{2J} + \frac{\Delta'}{2\Delta}\right)B \pm g_{\mathrm{eff}}\mu_B B, \tag{6}$$

and the slopes $d\omega_{\pm}/dB$ can differ in magnitude.

Such an exchange field in the ab plane coming from Ho spins polarized along the c axis can come from the Dzyaloshinskii-Moriya (DM) interaction, $H_{\mathrm{DM}} = \mathbf{D}\cdot(\mathbf{S}_{\mathrm{Ho}} \times \mathbf{S}_{\mathrm{Mn}})$, with a DM vector $\mathbf{D}$ in the ab plane [43,44]. Although we believe this DM term plays a role here, in the most straightforward scenario, this leads to the opposite effect: both AFR branches tilt up. To understand why, note that the effective exchange field $\mathbf{H}_{\mathrm{eff}} = -\mathbf{D} \times \langle \mathbf{S}_{\mathrm{Ho}} \rangle$ breaks the global symmetry of rotations in the ab plane manifest in the Hamiltonian (1). Mn spins orient themselves parallel to $\mathbf{H}_{\mathrm{eff}}$ to minimize the DM energy and select a ground state. In general, it is this change in the ground state with the change in field direction that leads to the nonanalyticity of the R and L excitations near $B = 0$. Deviations from these preferred directions now cost extra energy, which leads to a hardening of both AFR branches contrary to the experimental observations. We have found that other types of interactions breaking the global rotational symmetry that select a ground state generically harden both AFR branches [30]. In order to get a softening, one must have the combined effect of both DM interaction and quartic interactions that force an anisotropy in plane. For instance, the interaction

$$H_4 = K \sum_{\langle \mathrm{HoMn} \rangle} S^z_{\mathrm{Ho}} S^y_{\mathrm{Mn}} [3(S^x_{\mathrm{Mn}})^2 - (S^y_{\mathrm{Mn}})^2], \tag{7}$$

has been previously proposed to drive magnetic transitions in HMO [9]. However, other symmetry permitted quartic terms can also reproduce the observed asymmetry in the AFR (see Sec. III of the SM [30]). When both perturbations are present, one may select the ground state, and the other determines the stiffness of the hard modes resulting in a net softening. This is a generic mechanism that may lead to g-factor asymmetry in other systems as well.

In summary, high precision time-domain THz experiments uncovered an asymmetric splitting of an AFR of the Mn sublattice in the multiferroic HMO. Careful examination of the temperature dependence of this asymmetry unambiguously demonstrated the effect to be related to Ho-Mn interactions. Theoretical analyses found this asymmetry is only reproduced if quartic spin interactions between Ho-Mn moments are included in the spin Hamiltonian. One generally expects such interactions to be present in other hexagonal manganites with rare-earth magnetism. For instance, close inspection of the data of Ref. [29] reveals that the low energy branch of the AFR possesses a significantly larger g factor than the high energy branch in $TmMnO_3$, similar to our results in HMO. Our analysis suggests that such interactions may be a general feature of exceptionally low symmetry antiferromagnets and warrant consideration.

Research at Johns Hopkins University was funded by the U.S. Department of Energy, Office of Basic Energy Sciences, Division of Materials Sciences and Engineering through Grant No. DE-FG02-08ER46544. Work at Rutgers was supported by the Department Of Energy under Grant No. DOE: DE-FG02-07ER46382. N. J. L. acknowledges additional support through the Achievement Reward For College Scientists Foundation Dillon Fellowship. We would like to thank C. Broholm, M. Fiebig, R. Prasankumar, A. Sirenko, and D. Talbayev for helpful conversations.

[1] C. Kittel, Phys. Rev. **82**, 565 (1951).
[2] B. Lorenz, ISRN Condens. Matter Phys. **2013**, 497073 (2013).
[3] N. Hur, I. K. Jeong, M. F. Hundley, S. B. Kim, and S.-W. Cheong, Phys. Rev. B **79**, 134120 (2009).
[4] S. Nandi, A. Kreyssig, L. Tan, J. W. Kim, J. Q. Yan, J. C. Lang, D. Haskel, R. J. McQueeney, and A. I. Goldman, Phys. Rev. Lett. **100**, 217201 (2008).
[5] M. Fiebig, C. Degenhardt, and R. V. Pisarev, Phys. Rev. Lett. **88**, 027203 (2001).
[6] X. Fabrèges, I. Mirebeau, P. Bonville, S. Petit, G. Lebras-Jasmin, A. Forget, G. André, and S. Pailhès, Phys. Rev. B **78**, 214422 (2008).
[7] D. Talbayev, A. D. LaForge, S. A. Trugman, N. Hur, A. J. Taylor, R. D. Averitt, and D. N. Basov, Phys. Rev. Lett. **101**, 247601 (2008).
[8] D. Meier, H. Ryll, K. Kiefer, B. Klemke, J.-U. Hoffmann, R. Ramesh, and M. Fiebig, Phys. Rev. B **86**, 184415 (2012).
[9] S. G. Condran and M. L. Plumer, J. Phys. Condens. Matter **22**, 162201 (2010).
[10] T. Lottermoser, T. Lonkai, U. Amann, D. Holhwein, J. Ihringer, and M. Fiebig, Nature (London) **430**, 541 (2004).
[11] B. G. Ueland, J. W. Lynn, M. Laver, Y. J. Choi, and S.-W. Cheong, Phys. Rev. Lett. **104**, 147204 (2010).
[12] B. Lorenz, A. P. Litvinchuk, M. M. Gospodinov, and C. W. Chu, Phys. Rev. Lett. **92**, 087204 (2004).
[13] C. dela Cruz, F. Yen, B. Lorenz, Y. Q. Wang, Y. Y. Sun, M. M. Gospodinov, and C. W. Chu, Phys. Rev. B **71**, 060407 (2005).
[14] N. Iwata and K. Kohn, J. Phys. Soc. Jpn. **67**, 3318 (1998).
[15] F. Yen, C. R. dela Cruz, B. Lorenz, Y. Y. Sun, Y. Q. Wang, M. M. Gospodinov, and C. W. Chu, Phys. Rev. B **71**, 180407 (2005).
[16] K. Momma and F. Izumi, J. Appl. Crystallogr. **44**, 1272 (2011).
[17] S.-W. Cheong and M. Mostovoy, Nat. Mater. **6**, 13 (2007).
[18] B. B. Van Aken, T. T. M. Palstra, A. Filippetti, and A. Nicola, Nat. Mater. **3**, 164 (2004).
[19] C. J. Fennie and K. M. Rabe, Phys. Rev. B **72**, 100103 (2005).
[20] M. Fiebig, D. Fröhlich, K. Kohn, S. Leute, T. Lottermoser, V. V. Pavlov, and R. V. Pisarev, Phys. Rev. Lett. **84**, 5620 (2000).
[21] M. Fiebig, C. Degenhardt, and R. V. Pisarev, J. Appl. Phys. **91**, 8867 (2002).
[22] M. Fiebig, T. Lottermoser, and R. V. Pisarev, J. Appl. Phys. **93**, 8194 (2003).
[23] O. P. Vajk, M. Kenzelmann, J. W. Lynn, S. B. Kim, and S.-W. Cheong, Phys. Rev. Lett. **94**, 087601 (2005).
[24] P. J. Brown and T. Chatterji, J. Phys. Condens. Matter **18**, 10085 (2006).
[25] P. J. Brown and T. Chatterji, Phys. Rev. B **77**, 104407 (2008).
[26] H. Sugie, N. Iwata, and K. Kohn, J. Phys. Soc. Jpn. **71**, 1558 (2002).
[27] T. Lonkai, D. Hohlwein, J. Ihringer, and W. Prandl, Appl. Phys. A **74**, s843 (2002).
[28] W. Palme, F. Mertens, O. Born, and B. Lüthi, Solid State Commun. **76**, 873 (1990).
[29] E. C. Standard, T. Stanislavchuk, A. A. Sirenko, N. Lee, and S.-W. Cheong, Phys. Rev. B **85**, 144422 (2012).
[30] See Supplemental Material at http://link.aps.org/supplemental/10.1103/PhysRevLett.119.227601 for specific details of the crystal field spectra of HMO.
[31] N. J. Laurita, B. Cheng, R. Barkhouser, V. A. Neumann, and N. P. Armitage, J. Infrared, Millimeter, Terahertz Waves **37**, 894 (2016).
[32] N. P. Armitage, Phys. Rev. B **90**, 035135 (2014).
[33] P. Bowlan, S. A. Trugman, J. Bowlan, J.-X. Zhu, N. J. Hur, A. J. Taylor, D. A. Yarotski, and R. P. Prasankumar, Phys. Rev. B **94**, 100404 (2016).
[34] B. R. Judd, Proc. R. Soc. A **232**, 458 (1955).
[35] A. Abragam and B. Bleaney, *Electron Paramagnetic Resonance* (Clarendon Press, Oxford, 1970).
[36] R. J. Elliott and K. W. H. Stevens, Proc. R. Soc. A **218**, 553 (1953).
[37] S. Rosenkranz, A. P. Ramirez, A. Hayashi, R. J. Cava, R. Siddharthan, and B. S. Shastry, J. Appl. Phys. **87**, 5914 (2000).
[38] U. Ranon and K. Lee, Phys. Rev. **188**, 539 (1969).

[39] A. A. Sirenko, S. M. O'Malley, K. H. Ahn, S. Park, G. L. Carr, and S.-W. Cheong, Phys. Rev. B **78**, 174405 (2008).
[40] K. Stevens, Phys. Lett. **47A**, 401 (1974).
[41] R. C. Jones, J. Opt. Soc. Am. **31**, 488 (1941).
[42] C. M. Morris, R. V. Aguilar, A. V. Stier, and N. P. Armitage, Opt. Express **20**, 12303 (2012).
[43] I. Dzyaloshinsky, J. Phys. Chem. Solids **4**, 241 (1958).
[44] T. Moriya, Phys. Rev. **120**, 91 (1960).